Plant-expressed Hepatitis B core antigen virus-like particles: characterization and investigation of their stability in simulated and pig gastro-intestinal fluids

Alberto Berardi[1,2], *George P. Lomonossoff*[2], *David J. Evans*[2], *Susan A. Barker*[1*]

[1]School of Pharmacy, University of East Anglia, Norwich Research Park, Norwich, UK.

[2]Department of Biological Chemistry, John Innes Centre, Norwich Research Park, Norwich, UK

* Correspondence author

Current addresses:

Alberto Berardi, Faculty of Pharmacy, Applied Science Private University, Amman, Jordan

David J. Evans, School of Mathematics and Physical Sciences, University of Hull, Cottingham Road, Hull, HU6 7RX, UK

Susan A. Barker, School of Pharmacy, University College London, 29-39 Brunswick Square, London, WC1N 1AX, UK

Abstract

Virus-like particles (VLPs) are potential oral vaccine candidates, as their highly compact structure may allow them to withstand the harsh conditions of the gastro-intestinal (GI) environment. Hepatitis B core antigen (HBcAg) is an immunogenic protein that assembles into 30 or 34 nm diameter VLPs. Here, the stabilities of both the HBcAg polypeptide itself and the three-dimensional structure of the VLPs upon exposure to *in vitro* and *ex vivo* simulated gastric and intestinal fluids were investigated. Plant-expressed HBcAg VLPs were efficiently purified by sucrose density gradient and characterized. The purified VLPs did not show major chemical or physical instability upon exposure to the low pH conditions typically found in the stomach; however, they completely agglomerated upon acidification and subsequent pH neutralization. The HBcAg polypeptide was highly digested upon exposure to pepsin in simulated gastric fluids. HBcAg appeared more stable in both simulated and *ex vivo* intestinal fluids, where despite a partial digestion of the HBcAg polypeptide, the VLPs maintained their most immunogenic epitopes and their particulate conformation. These results suggest that HBcAg VLPs are likely to be unstable in gastric fluids, yet if the gastric instability could be bypassed, they could maintain their particulate structure and immunogenicity in intestinal fluids.

Keywords: HBcAg; VLPs; oral delivery; proteins; gastrointestinal fluids; gastrointestinal stability

1. Introduction

The mucosal delivery of protein-based therapeutics, including vaccines, is one of the greatest challenges of today's drug delivery research. For instance, in the case of the oral route, the harsh gastric and intestinal fluids pose severe obstacles to the stability of protein drugs (Lee, 2002). The first physicochemical barrier encountered in the gastro-intestinal (GI) tract is constituted by the stomach fluid: the pH in the stomach generally ranges from pH 1.0 to 2.5 in the normal fasted state condition (Evans et al., 1988). Furthermore, the stomach fluid is rich in the enzyme pepsin that constitutes a further biochemical barrier to proteins (Mahato et al., 2003). The intestine has a more neutral pH than the stomach, generally ranging from pH 6.3 to 7.5 (Evans et al., 1988). However, the intestinal fluid also represents a biochemical threat to the stability of therapeutic proteins, mainly due to the presence of pancreatic enzymes including trypsin and chymotrypsin (Mahato et al., 2003). In recent years, systems based on the use of nanoparticulate carriers, encapsulating and hence protecting labile proteins through their passage in the GI tract, have been investigated as possible options for the successful oral delivery of proteins (Kammona and Kiparissides, 2012).

Virus-like particles (VLPs) are viral mimics, whose structure resembles the antigenic conformation and repetitive nature of the whole virus from which they are derived, yet are non-infectious as they do not contain the viral genome (Jennings and Bachmann, 2008). VLPs differ from conventional nanoparticles, as the virus-derived protein antigen self-assembles into particles and hence the carrier is the antigen itself. Moreover, VLPs could be particularly suitable oral vaccine candidates, as it has been suggested that their highly compact structure could enable them to withstand the harsh GI environment (Herbst-Kralovetz et al., 2010; Huang et al., 2005).

61 For example, Norwalk VLPs, derived from Norwalk virus, a major pathogen responsible for
62 human gastro-enteritis, have been shown to be stable at low pH and are trypsin resistant (Ausar
63 et al., 2006).
64
65 Hepatitis B virus (HBV) is a major human pathogen. Chronic infection with HBV is associated
66 with cirrhosis and primary liver cancer. The 42 nm HBV virion is formed by an external
67 envelope surrounding an internal nucleocapsid, containing partially double-stranded DNA (Seitz
68 et al., 2007). This internal nucleocapsid results from the self-assembly of the nucleocapsid
69 protein, a 21 kDa protein called Hepatitis B core antigen (HBcAg): 180 or 240 HBcAg
70 monomers are arranged into 30 or 34 nm icosahedral particles (Birnbaum and Nassal, 1990;
71 Crowther et al., 1994). HBcAg VLPs can be produced as a recombinant protein in a variety of
72 hosts, including plants (Huang et al., 2006; Mechtcheriakova et al., 2006; Sainsbury and
73 Lomonossoff, 2008). HBcAg has been shown to induce potent B and T cell responses (Milich et
74 al., 1997, 1987). The very strong immunogenicity of HBcAg is believed to be related to its
75 particulate and polymeric nature. Over the years, HBcAg has also earned the reputation of being
76 an exceptionally promising carrier for foreign epitope sequences: the conjugation of such
77 epitopes to particulate carriers allows high density and repetitive display of these epitopes on the
78 surface of particles (Grgacic and Anderson, 2006). In addition, HBcAg is non-cytotoxic and is
79 well tolerated in humans (Whitacre et al., 2009).
80
81 In this study, HBcAg VLPs were produced in *Nicotiana benthamiana* using a transient
82 expression system (Sainsbury and Lomonossoff, 2008). The aim of this study was to investigate
83 both the chemical and physical stability of HBcAg VLPs upon exposure to several digestive and

84 denaturing conditions simulating the variable conditions of the GI environment. Such studies are
85 a prelude to the development of plant-HBcAg VLPs as a source of oral vaccines.
86
87 **2. Experimental Section**
88 **2.1. Materials**
89 pEAQ-*HT*-HBcAgΔ176 (Peyret et al., 2015a; Sainsbury et al., 2009) is a construct designed to
90 express the N-terminal 176 amino acids of HBcAg from the pEAQ transient expression vector.
91 Monoclonal mouse HBcAg antibody 10E11 was purchased from Abcam (UK). Anti-mouse HRP
92 conjugated antibody was obtained from Invitrogen (UK) or Amersham Bioscience (UK).
93 Complete® Protease inhibitor tablets were purchased from Roche (UK), Miracloth from Merck
94 (UK) and dialysis tubes from Spectrum Laboratories (Europe) or from Sigma -Aldrich (UK).
95 SDS-NuPAGE gels bis-tris Mini, NuPAGE MOPS buffer and NuPAGE LDS Sample Buffer
96 were purchased from Invitrogen (UK). β-Mercaptoethanol, Brilliant Blue R Concentrate,
97 3,3',5,5'-tetramethylbenzidine dihydrochloride (TMB) substrate were purchased from Sigma
98 (UK). InstantBlue stain was bought from Expedon (UK), SuperSignal West Dura
99 Chemiluminescent Substrate from Thermo Scientific (UK) and polyvinylidene fluoride (PVDF)
100 membranes and Hyperfilm from Amersham (UK). Pepsin (Ph Eur) from porcine gastric mucosa
101 and pancreatin (≥ 3× USP) from porcine pancreas were purchased from Sigma-Aldrich (UK). A
102 full-length intestine was obtained from a freshly killed pig at a local abattoir (H. G. Blake,
103 Costessey Ltd, Norwich, UK). The animal was processed under standard UK legislation for
104 food-producing animals, the intestine extracted within a few hours of slaughter, transported
105 intact to the laboratory on ice and the intestinal fluids extracted within a short time.
106

2.2. HBcAg VLP expression, purification and characterization

2.2.1. Plant growth, protein expression, extraction and detection techniques

Nicotiana benthamiana plants were grown in a glasshouse at a fixed temperature of 25 ºC and used 3 to 4 weeks after pricking out. Suspensions of *Agrobacterium tumefaciens* (strain LBA 4404) containing pEAQ-*HT*-HBcAgΔ176 were pressure-infiltrated into *N. benthamiana* leaves, using needle-less syringes as described previously [20]. Infiltrated leaves were harvested 6 to 7 days post-infiltration. Extraction of the protein from the leaves was performed at 4 ºC by homogenisation in three volumes of extraction buffer 1 (50 mM Tris-HCl, pH 7.25 : 150 mM NaCl, 2 mM ethylenediaminetetraacetic acid (EDTA), 0.1% w/v Triton X-100, 1 mM dithiothreitol and Complete® tablet) or extraction buffer 2 (10 mM Tris-HCl, pH 8.4 : 120 mM NaCl, 1 mM EDTA, 0.75% w/v sodium deoxycholate, 1 mM dithiothreitol and a Complete® Protease inhibitor tablet). The whole extract was then passed through a double layer of Miracloth and subsequently clarified by centrifugation at 12,000 x g in order to remove most plant cell debris. All extractions were performed at 4 ºC. Plant expressed HBcAg VLPs were further purified by centrifugation of the protein extracts on 10-60% w/v sucrose density gradients prepared in 10 mM Tris-HCl pH 8.4, 120 mM NaCl. The gradients were centrifuged for 2.5 hours at 4°C at either 40,000 rpm in a SW41Ti rotor or at 30,000 rpm in a Surespin 630 rotor. After centrifugation, the gradients were fractionated and the fractions dialysed against 10 mM Tris-HCl, 120 mM NaCl, pH 8.4 or phosphate buffer saline (PBS).

2.2.2. Sodium Dodecyl Sulfate Polyacrylamide Gel Electrophoresis (SDS-PAGE) - Coomassie Blue Staining

Proteins were reduced and denatured by adding one volume of 3X LDS β-mercaptoethanol to two volumes of the samples. Samples were then heated to 100 ºC for 5 minutes. NuPAGE gels were run in 3-(*N*-morpholino)propanesulfonic acid (MOPS) buffer following the manufacturer's instructions. After electrophoresis, the protein bands were visualised by addition of Coomassie blue-protein stain for at least 1 hour.

2.2.3. Dot blot

Three µL of each sample were spotted onto PDVF membranes using 10 µL tips. Membranes were left to dry for 30 minutes and then blocked with the blocking buffer (5% w/v dried milk, 0.1% v/v Tween 20 in PBS) at 4 ºC overnight, before being incubated with monoclonal mouse HBcAg antibody, diluted 1:5000 in dot blot blocking buffer, for 2 hours. The membranes were then probed with anti-mouse horseradish peroxidase (HRP) conjugated secondary antibody, diluted 1:5000 in blocking buffer for a further 2 hours. Chemiluminescent HRP substrate was used for the detection of the secondary antibody and captured on Hyperfilm (Sainsbury and Lomonossoff, 2008).

2.2.4. Western blot

SDS-PAGE gels were run as described above and the proteins transferred to PVDF membranes immediately after the electrophoresis. The membranes were blocked with the blocking buffer (1% w/v bovine serum albumin, 1% w/v casein, 0.05% v/v Tween 20 in PBS) at 4 ºC overnight and before being incubated with anti-mouse horseradish peroxidase (HRP) conjugated secondary antibody, diluted 1:5000 in blocking buffer for 2 hours. Chemiluminescent HRP substrate was

151 used for the detection of the secondary antibody and captured on Hyperfilm (Peyret et al., 2015a;
152 Sainsbury and Lomonossoff, 2008).
153
154 **2.2.5. Transmission Electron Microscopy (TEM)**
155 Samples diluted to an approximate concentration of 0.1 mg/mL were adsorbed onto hexagonal,
156 plastic and carbon-coated copper grids, which were then washed three times with water. The
157 grids were negatively stained with 2% w/v uranyl acetate before being imaged using a FEI
158 Tecnal G2 20 Twin TEM with a built-in digital camera.
159
160 **2.2.6. Native agarose gel electrophoresis**
161 Agarose gels [1.2% w/v agarose in Tris/Borate/EDTA (3.03 g/L Tris-HCl, 5.5 g/L boric acid, 2
162 mM EDTA)] were usually run in duplicate at 60 V for 90 minutes (Aljabali et al., 2012). One gel
163 was stained with a 0.5 µg/mL solution of ethidium bromide for 30 minutes and then visualised
164 under UV light (wavelength = 302 nm). The other gel was stained with Brilliant Blue R
165 Concentrate (Coomassie stain) for 30 minutes.
166
167 **2.3. HBcAg Stability in Simulated Gastric Fluid (SGF)**
168 **2.3.1. HBcAg Stability in Simulated Gastric Fluid (SGF) without Pepsin**
169 VLP-rich fractions corresponding to 30 and 40 % w/v sucrose density bands were pooled
170 together and were then diluted 1:5 with a solution of 80 mM HCl and 34 mM NaCl, resulting in a
171 final pH of 1.2, matching SGF (British Pharmacopeia, 2012). The HBcAg solution in SGF was
172 incubated at 37 °C for two hours. After incubation, it was layered on the top of a pH 1.2, 10 to
173 45% w/v sucrose density step gradient. Alternatively, purified HBcAg VLP preparations were

incubated at pH 1.2 for two hours as described previously. At the end of the two hour incubation, the pH of the sample was neutralised by initial dropwise addition of 1 M NaOH. The neutralising agent was switched to 0.1 M NaOH once the pH became closer to neutrality. The sample was then layered on the top of 10 mM Tris-HCl, 120 mM NaCl pH 8.4, 10 to 45% w/v sucrose density step gradient. As a control, the purified HBcAg particles were diluted in a 10 mM Tris-HCl pH 8.4, 120 mM NaCl solution. After two hours incubation, the control sample was layered on the top of a 10 mM Tris-HCl pH 8.4, 10 to 45% w/v sucrose density step gradient. Following ultracentrifugation, fractions were collected from the sucrose gradients and analysed by Coomassie stained SDS-PAGE. If a precipitate formed at the bottom of the tube upon ultracentrifugation, it was re-suspended in 10 mM Tris-HCl, 120 mM NaCl pH 8.4 and analysed by Coomassie stained SDS-PAGE and Western blot.

For native agarose gel analysis, purified HBcAg VLPs in water were diluted 1:4 in each of the four acidic solutions: 10 mM HCl (pH 2) with 34 mM NaCl, 3.2 mM HCl (pH 2.5) with 34 mM NaCl, 1 mM HCl (pH 3) with 34 mM NaCl and 0.32 mM HCl (pH 3.5) with 34 mM NaCl. After two hours incubation, the four samples were loaded on agarose gel for electrophoresis. For TEM analysis, purified HBcAg VLPs in water were diluted 1:6 with a solution of 73 mM HCl to a final pH of 1.2. After two hours incubation at 37 °C, the pH was neutralised using aliquots of 400 mM $NaHCO_3$. The resulting sample was used for imaging.

2.3.2. HBcAg Stability in Simulated Gastric Fluid (SGF) with Different Pepsin Concentrations

196 Purified HBcAg VLPs were incubated at pH 1.2 with different concentrations of pepsin and a
197 control with no pepsin (10, 3.2, 1, 0.5, 0.2, 0.1, 0.05, 0.01 and 0 mg/mL). After two hours
198 incubation at 37 ºC, the samples were boiled to stop the enzymatic reaction and the proteins
199 analysed by Western blotting.
200
201 **2.4. HBcAg Stability in in vitro and ex vivo Intestinal Fluid**
202 **2.4.1. HBcAg Stability in Simulated Intestinal Fluid (SIF)**
203 Simulated intestinal fluid (SIF) with pancreatin was prepared by mixing 7.7 mL of 0.2 M
204 NaOH with 25 mL of a solution containing 6.8 g of K_2PO_4 and 50 mL of water. Porcine
205 pancreatin (≥ 3× USP), 333 mg, was then added. The pH was then adjusted to 6.8 and the
206 volume diluted to 100 mL with water (British Pharmacopeia, 2012). SIF without pancreatin was
207 prepared identically, but omitting the pancreatin. Before the stability experiment, a protease
208 inhibitor tablet was diluted in 5 mL SIF without pancreatin. For Coomassie stained SDS-PAGE
209 and Western blot analysis, five samples of purified HBcAg diluted 1:19 in SIF were incubated at
210 37 ºC for 240, 180, 120, 60 and 30 minutes. After the incubation the (10 x) protease inhibitor
211 solution was diluted 1:9 in each digestion sample to stop the enzymatic reaction and samples
212 were immediately cooled on ice. A 1:19 dilution of HBcAg in SIF without pancreatin was used
213 as a positive control. A 1:19 dilution of water in SIF was used as a negative control. All samples
214 were analysed by Coomassie stained SDS-PAGE and Western blotting.
215
216 For dot blot analysis, the sample resulting from the digestion and the positive control were
217 loaded onto six different 10-60% w/v sucrose density gradients. After ultracentrifugation,
218 fractions from the sucrose gradients were collected and subjected to dot blot analysis.

For native agarose gel electrophoresis, purified HBcAg was diluted 1:9 in SIF and incubated at 37º C for 30, 60, 120, 180 or 240 minutes. After the incubation the protease inhibitor solution was diluted 1:9 in each sample corresponding to different incubation times and they were immediately cooled on ice. A 1:9 dilution of HBcAg in SIF without pancreatin was used as positive control and a 1:9 dilution of water in SIF was used as a negative control. All samples were used for ethidium bromide stained and Coomassie stained agarose gel electrophoresis.

For TEM imaging, HBcAg was diluted 1:6 in SIF and the sample was incubated for 120 minutes. The enzymatic reaction was then stopped by 1:9 dilution of protease inhibitor solution in the digestion sample. The sample was kept cool on ice. TEM imaging was carried out within two hours of the end of the incubation.

2.4.2. Ex Vivo HBcAg Stability in Natural Intestinal Fluid (natIF)

Pig intestinal fluids were chosen as natural intestinal fluids (natIFs). The full-length intestine collected from the freshly killed animal was immediately transported to the laboratory and used for the collection of the luminal fluids. Four segments of approximately the same size from the proximal to the distal small intestine were divided and luminal fluid content was collected from each of the four segments separately. Small aliquots were made and frozen at – 80 ºC until use. Digestion experiments were conducted within ten weeks of collection of the fluids. For the SDS-PAGE analysis, aliquots from the four different segments of the small intestine were thawed and the solid content was pelleted by centrifugation at 9300 x g for 10 minutes. Aliquots from the most proximal part of the intestine (i.e. duodenum) were centrifuged twice to separate the more

viscous phase. The supernatants constituted the natural intestinal fluid (natIF) of this study. The four natIFs from the proximal to the distal small intestine are referred to as natIF 1, natIF 2, natIF 3 and natIF 4 for the studies detailed below. Purified HBcAg aliquots were diluted 1:19 in each of the four natIFs and incubated at 37 ºC for 4 hours. At the end of the incubation, 1:3 dilutions of the four samples in water where made and then boiled to stop the enzymatic reaction. For a positive control, HBcAg aliquots were diluted 1:19 in PBS. Moreover, enzymatically inactive natIFs media were also used as positive controls: 1:3 dilutions of the natIFs in water and LDS β-mercaptoethanol were boiled for 10 minutes and then cooled and purified HBcAg was added in the same ratio as in the digestion samples. Negative controls were also created by diluting the PBS in natIFs. All samples were then analysed by Coomassie staining SDS-PAGE and Western blot.

For dot blots, purified HBcAg aliquots were diluted 1:19 in the four natIFs and incubated at 37 ºC for four hours. Then the proteolysis was stopped by the addition of 1:9 dilution of protease inhibitor solutions. For a positive control, HBcAg was diluted 1:19 in PBS. The control and the digestion samples were loaded onto five identical sucrose density gradients. After ultracentrifugation, fractions from the sucrose gradients were collected and analysed by dot blot using anti-HBcAg mouse monoclonal antibody.

3. Results and Discussion

3.1 Purification and analysis of plant-expressed HBcAg

Sainsbury and Lomonossoff [14] showed that HBcAg could be expressed using the CPMV-*HT* system up to yields of approximately 1 g per kg of fresh weight tissue. Subsequently methods for

265 the efficient purification of plant-expressed HBcAg VLPs have been developed (Peyret, 2015;
266 Peyret et al., 2015a, 2015b). Here, the final purification of VLPs from the crude extract was
267 carried out by sucrose density gradient ultracentrifugation. Seven fractions, each approximately
268 corresponding to the density layers of sucrose and to the supernatant, were collected from the
269 bottom of the tube (Figure 1. A) and analysed by Coomassie stained SDS-PAGE and Western
270 blot (Figure 1. B left and right side, respectively).
271
272 The Coomassie stained gel (Figure 1. B left side) showed a 20 kDa band, corresponding to the
273 size of the 176 amino acid long monomeric HBcAg, in the 30, 40 and 50% w/v sucrose gradient
274 fractions. The same band was, however, absent from the 60% w/v sucrose fraction. Most plant
275 protein bands remained in the supernatant and in the 10 and 20% w/v sucrose fractions. The anti-
276 HBcAg Western blot (Figure 1. B right side) confirmed that the 20 kDa band, detected in the 30,
277 40 and 50 % w/v sucrose fractions in the Coomassie stained SDS-PAGE gel, corresponded to
278 HBcAg. As expected, HBcAg was also detected in the original crude extract (lane E). In the
279 HBcAg-rich lanes, it is also possible to notice a persistent 40 kDa band. The band was also
280 observed by others and corresponds to HBcAg dimers, which are resistant to denaturation
281 (Huang et al., 2006; Mechtcheriakova et al., 2006). Even larger size HBcAg multimeric
282 structures have been detected in denaturing gel electrophoresis (Broos et al., 2007). Weaker
283 bands of *circa* 15 kDa monomeric HBcAg and its dimer of 30 kDa can also be seen and they are
284 possibly the result of partial enzymatic digestion of HBcAg by plant proteins.
285
286 These results are in accordance with previous studies on HBcAg (Birnbaum and Nassal, 1990;
287 Broos et al., 2007; Huang et al., 2006). Furthermore, when a sample containing the dialysed 30

and 40% w/v sucrose gradient fractions was examined by native agarose gel (Figure 1. C), a clear band could be seen in the both the Coomassie- and ethidium bromide-stained gels. The two signals had the same electrophoretic mobility, suggesting that the VLP protein core, stained by the Coomassie, encapsidated nucleic acids, stained by ethidium bromide, consistent with previous reports (Newman et al., 2003). The presence of intact VLPs was further confirmed by TEM images (Figure 1. D) of the dialysed 30 and 40% w/v sucrose gradient fractions: intact VLPs were clearly visible and their diameter (*circa* 30 to 35 nm) matches the size documented in the literature (Lee and Tan, 2008; Wingfield et al., 1995). Overall, the Coomassie-stained SDS-PAGE gel, the native agarose gel and the TEM showed a very high degree of purification of the VLPs upon ultracentrifugation. Approximately, a purity of > 90% could be estimated by visualization of the Coomassie-stained gel (Figure 1 B left side, lanes 4 and 5).

301

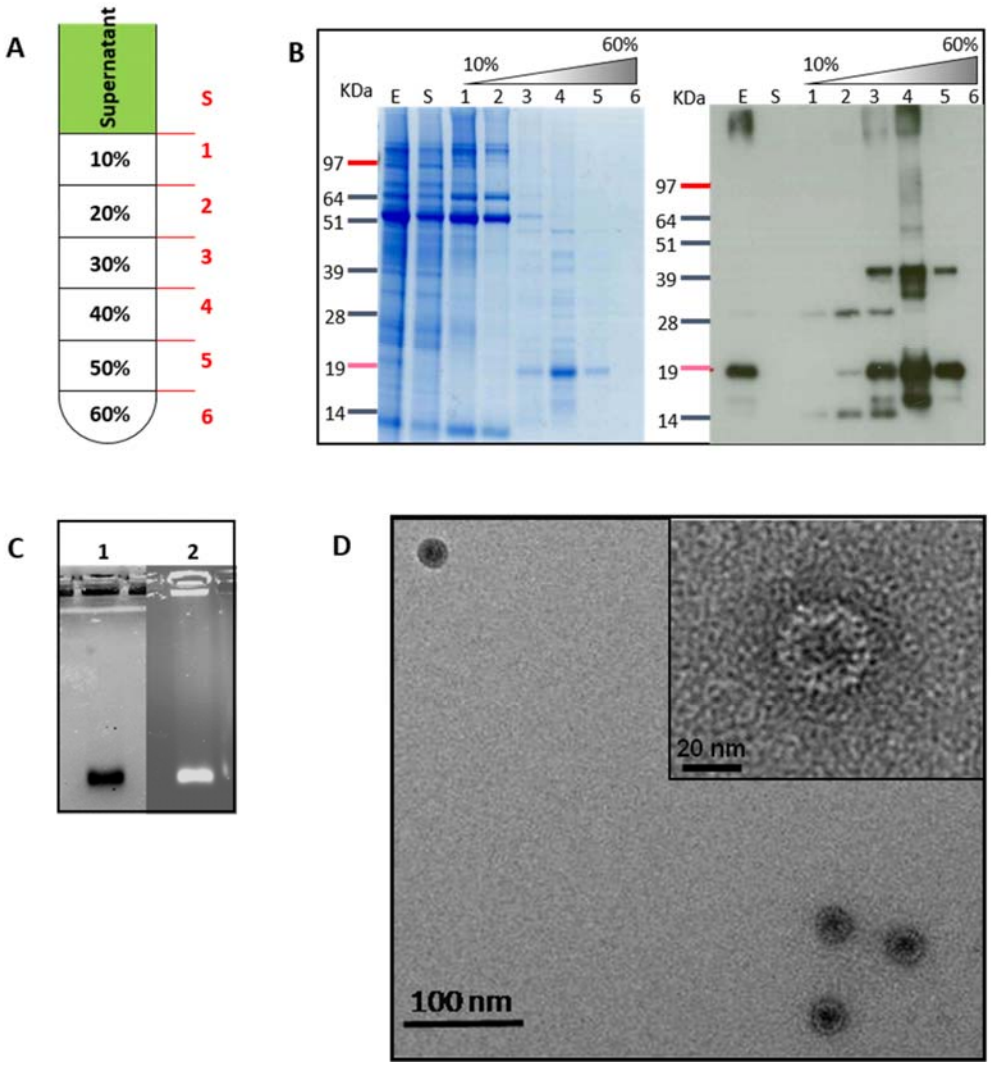

302

303

304 Figure 1. HBcAg purification and characterization. (A) Diagram of sucrose gradient (7 fractions
305 from the supernatant to 60% w/v sucrose); (B) Coomassie stained SDS-PAGE (left side) and
306 Western blot (right side) of the fractions. The lanes arrangement was as follows: crude extract
307 (lane E), supernatant (lane S), 10 to 60% w/v sucrose fractions (lane 1 to lane 6). (C) Native
308 agarose gel electrophoresis - stained with Coomassie stain (lane 1) or with ethidium bromide

309 (lane 2); and (D) TEM images of Purified HBcAg samples, dialysed from 30 and 40% w/v
310 sucrose gradient fractions.

311

312 **3.2. HBcAg in vitro and ex-vivo stability in gastro-intestinal media**

313 A previous study on plant-expressed HBcAg VLPs showed that oral administration of plant
314 extracts containing HBcAg elicited only poor immunogenicity in mice and it was speculated that
315 this could have been due to the gastric degradation or the physical disassembly of the antigen
316 (Huang et al., 2006). Hence, the stability of plant-expressed HBcAg VLPs in gastric and
317 intestinal conditions was investigated here: each experiment consisted of incubation of purified
318 VLPs in the bio-relevant media, followed by a post-incubation assessment of their physical and
319 chemical stability.

320

321 **3.2.1. HBcAg Stability in Simulated Gastric Fluid (SGF)**

322 Initially the stability of plant-expressed HBcAg VLPs was investigated at the acidic pH of the
323 SGF (pH 1.2). Three experiments were carried out (
324 Figure 2. A, B and C): in one case purified HBcAg VLPs were incubated for 2 hours at pH 8.4
325 and then separated by sucrose gradient ultracentrifugation, with fractions of the gradient
326 prepared at the same pH (control,
327 Figure 2. A). In the second case HBcAg VLPs were incubated for 2 hours at pH 1.2 and then
328 sample separated by sucrose gradient ultracentrifugation, set up in a way to maintain the pH of
329 the sucrose fractions consistent with the incubation pH (

330 Figure 2. B). In the third case, HBcAg VLPs were incubated for 2 hours at pH 1.2, then,
331 following neutralization, the sample was separated by sucrose gradient ultracentrifugation, with
332 sucrose fractions prepared at pH 8.4 (
333 Figure 2. C).
334
335 SDS-PAGE followed by Coomassie Blue staining of the collected fractions shows that the
336 acidic pH of the SGF did not chemically degrade the HBcAg polypeptide, which ran as a *circa*
337 20 kDa protein band (
338 Figure 2. B), as in the control (
339 Figure 2. A). HBcAg migrated towards the bottom of the density gradient in the control sample
340 incubated at pH 8.4 (
341 Figure 2. A), as indicated by the presence of the 20 kDa band only in the lanes corresponding
342 to 30 and 40% w/v sucrose fractions (lanes 6 to 8), suggesting physically intact VLPs. However,
343 in the sample incubated in SGF and analysed on a sucrose gradient at pH 1.2 (
344 Figure 2. B), the 20 kDa band could be seen in most of the fractions (lanes 1 to 8). This result
345 clearly suggests that the capsid structure of HBcAg VLP exhibits a certain degree of physical
346 instability on exposure to the acidic conditions. In the case of the sample of VLPs initially
347 exposed to pH 1.2 and then neutralized and separated by ultracentrifugation containing fractions
348 at pH 8.4, the Coomassie stained gel (
349 Figure 2. C) showed that a 20 kDa protein band, corresponding to HBcAg, was not present in
350 any of the gradient fractions.
351

352 However, a precipitate was visible at the bottom of the tube used for the ultracentrifugation of
353 the sample. This precipitate was re-suspended and analysed by SDS-PAGE, revealing the
354 presence of a band of a similar size to HBcAg, which reacted with anti-HBcAg antibodies in a
355 Western blot (Fig. 2C). The fact that HBcAg was not found in any of the fractions of the gradient
356 but in a precipitate at the bottom of the tube indicates that HBcAg was not present as intact VLP,
357 nor as a disassembled monomeric or multimeric form but as a high molecular weight aggregate.
358
359 For a final characterisation of HBcAg in SGF without pepsin, purified HBcAg particles were
360 incubated in SGF at pH 1.2 for two hours and then the acidity was neutralised. This sample was
361 used for TEM imaging. The TEM image (
362 Figure 2. D) showed that the typical HBcAg VLPs detected in the control sample could not be
363 found in the acidified and neutralised sample; instead aggregates could be seen, probably
364 representing aggregated VLPs.
365

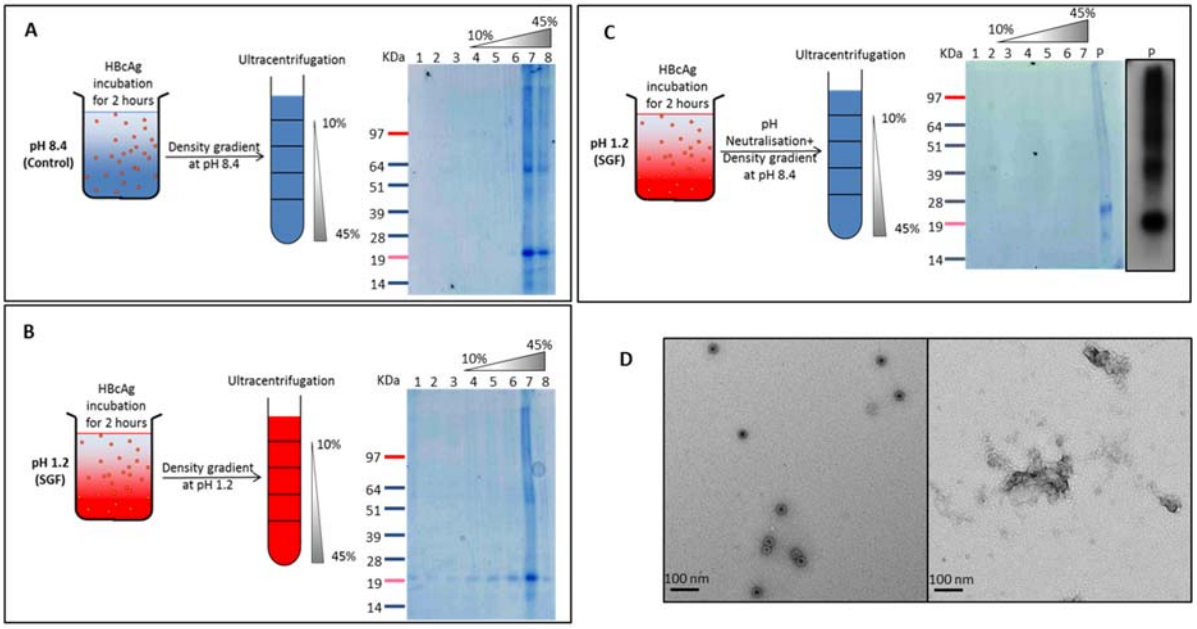

Figure 2. HBcAg stability in simulated gastric fluid (without pepsin). (A) Purified HBcAg was incubated in the control (pH 8.4) and then after 2 hours incubation, separated by density gradient ultracentrifugation at pH 8.4 - supernatant (lanes 1 to 3), 10 to 45% w/v sucrose fractions (lanes 4 to 8). (B) Purified HBcAg was incubated in SGF (pH 1.2) and then, after 2 hours incubation, separated by density gradient ultracentrifugation at pH 1.2 - supernatant (lanes 1 to 3), 10 to 45% w/v sucrose fractions (lanes 4 to 8). (C) Purified HBcAg was incubated in SGF (pH 1.2) and then after 2 hours incubation, the pH was neutralized and the sample separated by density gradient ultracentrifugation at pH 8.4 - supernatant (lane 1), 10 to 45% w/v sucrose fractions (lanes 2 to 7); precipitate (lane P); at the right side of the image the same precipitate was examined by Western blot. (D) TEM images: a control HBcAg sample (left image), an HBcAg sample after 2 hours acidification in SGF and subsequent neutralisation (right image).

These results taken together indicate that the HBcAg polypeptide is chemically stable at pH 1.2. However, the VLPs tend to partially disassemble at this pH (

Figure 2. B). When the pH is raised the dissociated subunits tend to form aggregates rather than reassemble into VLPs. (

Figure 2. C and D). These results demonstrate that HBcAg VLPs are likely to be physically unstable in the stomach environment of humans. Although it is possible that the low pH would not cause a complete disassembly of the capsid, the subsequent passage to a more neutral pH in the intestine would induce aggregation. However, the actual pH of human gastric fluid in fasted state is not strictly 1.2, but is in the range between 1.0 and 2.5 (Evans et al., 1988). Hence, to better delineate HBcAg VLP physical stability in gastric conditions, the threshold pH for HBcAg VLP stability was investigated using native agarose gel electrophoresis.

The ethidium bromide-stained agarose gel (Figure 3. - left side) showed the presence of nucleic acids trapped in the wells of samples incubated at pH 2.0 (lane 1) and pH 2.5 (lane 2). The sample incubated at pH 3.0 (lane 3) showed a smear of nucleic acids in the gel, while a discrete band was visible in the sample incubated at pH 3.5 (lane 4). The Coomassie stained gel (Figure 3. - right side) confirmed the presence of a protein smear in the sample incubated at pH 3 (lane 3); furthermore, a protein band could be seen in the sample incubated at pH 3.5 (lane 4): this band showed an identical electrophoretic migration to the respective lane in the ethidium bromide gel. These results suggest that HBcAg VLP quaternary structure is physically stable upon incubation in acid at pH 3.5 for two hours but is only partially stable when incubated at pH 3.0. Considering the previous finding that HBcAg VLPs appeared to partially dissociate and then aggregate upon acidification and subsequent neutralisation (

Figure 2. C and D), it is likely that HBcAg VLPs treated at pH 2.0 and pH 2.5 underwent a similar process upon neutralisation by the Tris/Borate/EDTA (TBE) buffer present in the gel, leading to observed trapping in the wells.

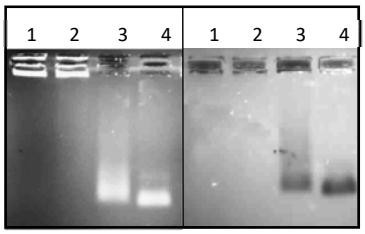

Figure 3. HBcAg VLP stability in different acidic conditions. HBcAg was incubated at different pH and the samples run in an ethidium bromide stained native agarose gel (left) and an identical Coomassie stained gel (right): pH 2 (lane 1); pH 2.5 (lane 2); pH 3 (lane 3) and pH 3.5 (lane 4).

This result is in accordance with Newman et al [25]: in that case, it was shown that bacterially expressed HBcAg incubated at pH 2.0 for only 30 minutes was unstable and it remained blocked in the well (Newman et al., 2003). Overall, in the current study, the native agarose gel electrophoresis revealed that this complete loss of the physical stability upon incubation of HBcAg for two hours in acid and further neutralisation occurs at pH values below 3 to 3.5 (Figure 3). The fact that the VLP particulate structure was lost upon incubation in media at pH values lower than pH 3 to 3.5 suggests that HBcAg would be unstable in the fasted gastric environment, i.e. pH 1 to pH 2.5 (Evans et al., 1988). However, it was reported that the average stomach pH can remain > 3.5 for the first three hours after a meal (Kalantzi et al., 2006). Therefore, it could be expected that the VLP structure could be physically stable at the pH of the fed stomach.

The stability of purified plant-expressed HBcAg was also evaluated after 2 hours incubation in SGF in the presence of the enzyme pepsin. The British Pharmacopoeia (2012) formula of SGF has a fixed 3.2 g/L pepsin (Ph Eur) concentration; however variations of pepsin activity up to four orders of magnitude have been reported in humans (Gomes et al., 2003). For this reason it was decided to incubate several aliquots of HBcAg in SGF at pH 1.2 containing pepsin at concentrations ranging from 10 g/L to 0.01 g/L. After two hours incubation, the samples were analysed by Western blotting (Figure 4.). The Western blot shows that the 20 kDa band, present in the control and corresponding to intact HBcAg, was absent in the sample of HBcAg incubated in SGF containing 3.2 g pepsin/L, i.e. the concentration specified in the British Pharmacopoeia (2012). Furthermore, some digestion of HBcAg occurred at all concentrations of pepsin. For concentrations of pepsin ≥ 0.5 g/L (lanes 2 to 5), no anti-HBcAg signal could be detected; however, for concentrations of pepsin ≤ 0.2 g/L (lanes 7 to 10) a *circa* 14 kDa band of anti-HBcAg immunoreactivity could be visualised. Only when the concentration of pepsin was as low as 0.01 g/L (lane 10) was a detectable amount of 20 kDa HBcAg present.

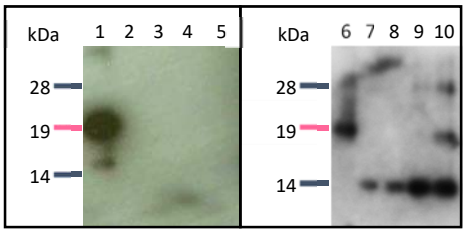

Figure 4. HBcAg digestion in SGF (with pepsin). HBcAg was incubated for two hours in SGF containing different concentrations of pepsin. The digested samples were then analysed by Western blot: SGF without pepsin (lane 1 and lane 6); 10 g/L pepsin (lane 2); 3.2 g/L pepsin (lane 3); 1 g/L pepsin (lane 4); 0.5 g/L pepsin (lane 5); 0.2 g/L pepsin (lane 7); 0.1 g/L pepsin (lane 8); 0.05 g/L pepsin (lane 9) and 0.01 g/L pepsin (lane 10).

This result suggests that HBcAg is extremely sensitive to chemical digestion by pepsin, not only at the pharmacopoeial pepsin concentration of SGF, but at thousands-fold lower concentrations. Wang et al (2015) have recently shown that there is a good correlation between the stability of peptides in SGF and native human gastric fluids. Hence, according to the data presented here, it is likely that HBcAg, aside from being physically unstable, would also be highly digested in the gastric fluid *in vivo*.

3.2.2 HBcAg in Intestinal Fluids: An *In Vitro* and *Ex Vivo* Stability Approach

The second barrier that HBcAg will encounter upon oral administration is the harsh environment of the small intestine: it contains several enzymes, including trypsin and chymotrypsin, which could digest a protein antigen. The ability of HBcAg to withstand the intestinal digestive environment was investigated from two angles: firstly HBcAg was incubated in a conventional *in vitro* model of intestinal fluid containing pancreatic enzymes. Then a more bio-relevant study was carried out using natural small intestinal fluids from pig, in order to more closely mimic the *in vivo* scenario in humans. Similar trends in the degradation of peptides in native human intestinal fluids, native pig intestinal fluids and simulated human intestinal fluids were observed by Wang et al (2015), validating the approach used.

The results of the experiments examining the chemical and physical stability of HBcAg VLPs incubated in SIF are shown in Figure 5. The Coomassie stained gel (Figure 5. A) shows that the *circa* 20 kDa band, seen in the positive control (lane 1) and corresponding to HBcAg, slightly overlaps with a much fainter band of the same size in the negative control (lane 2). For this

466 reason, careful consideration is required when interpreting these results. The different protein
467 bands visible in the negative control are probably pancreatic proteins and enzymes. At all
468 incubation times in SIF, HBcAg was partially digested to give predominantly a *circa* 17 kDa
469 protein band. The intensity of this band seems to increase proportionally with the incubation time
470 in SIF. These results were confirmed by the Western blot, which shows that the strongest anti-
471 HBcAg signal in the samples incubated in SIF (lanes 3 to 7) was the *circa* 17 kDa band, though a
472 series of HBcAg-specific bands of intermediate sizes between the full-length and the 17 kDa
473 version were also present in smaller quantities. As expected a *circa* 20 kDa band, corresponding
474 to undigested HBcAg is seen in the positive control (lane 1) and no bands are present in the
475 negative control (lane 2). Considering that the anti-HBcAg mouse monoclonal primary antibody
476 used has specificity for the first 10 amino acids at the N-terminal, it is evident that the digestion
477 is expected to have only occurred at the C-terminus. In contrast, digestion at the N-terminal
478 would have resulted in loss of affinity of HBcAg to this given antibody, resulting in a lack of
479 immunoreactivity. The above results demonstrated that HBcAg was digested to a smaller protein
480 after exposure to SIF.
481
482 To determine whether the major digestion product (17 kDa) was in the form of VLPs, the
483 digested samples were examined on sucrose gradients. Figure 5. C, D and E illustrate the effect
484 of the incubation of HBcAg in SIF with pancreatin on its physical stability. The dot blot (Figure
485 5. C) represents the HBcAg sedimentation upon ultracentrifugation of the samples undergoing
486 the proteolytic treatment. Irrespective of the incubation time in SIF with pancreatin, most
487 HBcAg immunoreactivity could be visualised in dots corresponding to the 30 and 40% w/v
488 sucrose fractions, as in the undigested VLP positive control. This result suggests that HBcAg

maintained its particulate form after digestion. This was also confirmed by native agarose gel electrophoresis (Figure 5. D). HBcAg incubated in SIF (lanes 2 to 7) showed electrophoretic migration almost identical to that of the untreated VLP of the control sample (lane 1). Finally, TEM imaging (Figure 5. E) showed that VLPs were still present after incubation of HBcAg in SIF with pancreatin for 120 minutes. These results taken together indicate that HBcAg was partially digested upon treatment in SIF; however the digestion did not seem to interfere with physical stability of the VLPs.

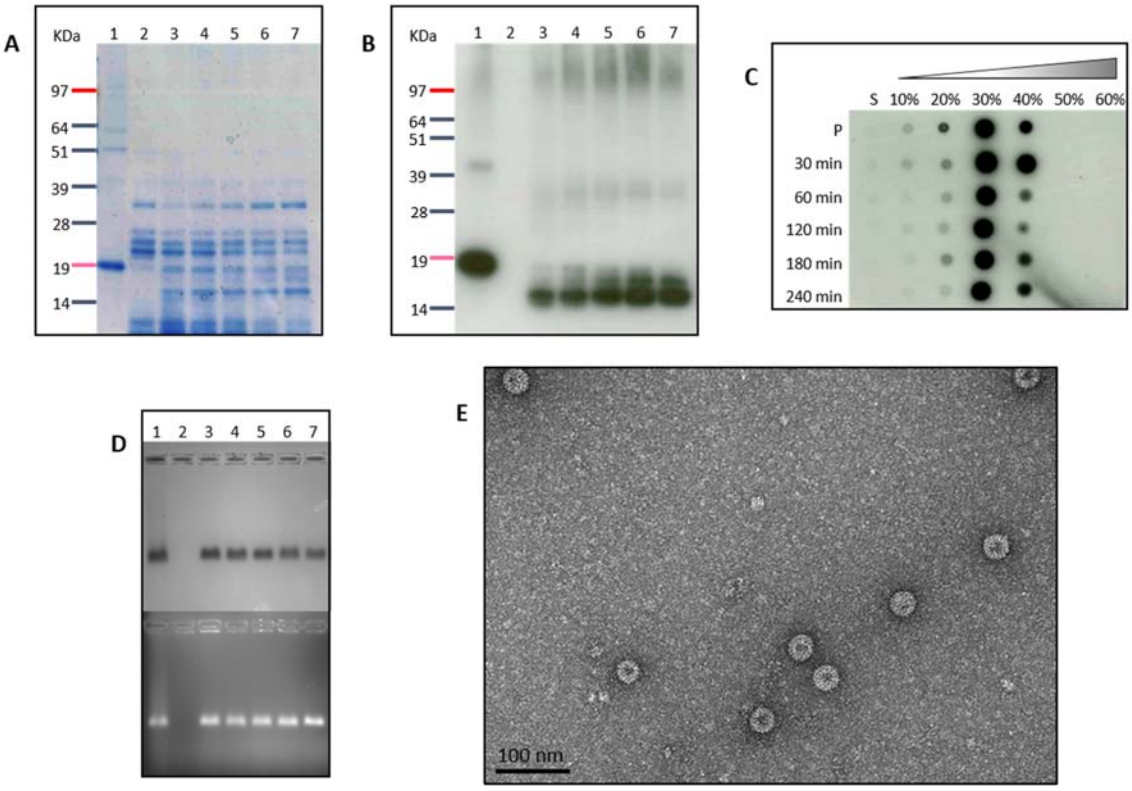

Figure 5. HBcAg chemical stability in SIF. Aliquots of purified HBcAg were incubated in SIF with pancreatin for different time intervals. All the resulting digestion samples were analysed by different techniques. (A) Coomassie stained SDS-PAGE and (B) Western blot: positive control

(lane 1); negative control (lane 2); 30 minutes digestion (lane 3); 60 minutes (lane 4); 120 minutes (lane 5); 180 minutes (lane 6); 240 minutes (lane 7). (C) Dot blot of sucrose gradient fractions: percentages indicate the approximate concentration of the sucrose density fraction (S = supernatant), while incubation times are listed vertically; (P = positive control). (D) Native agarose gel of the digested samples : positive control (lane 1); negative control (lane 2); 30 minutes (lane 3); 60 minutes (lane 4); 120 minutes (lane 5); 180 minutes (lane 6); 240 minutes (lane 7). (E) TEM image of HBcAg incubated in SIF with pancreatin for two hours.

The pancreatin present in the SIF contains several pancreatic proteases, including trypsin, chymotrypsin and elastase, which could potentially digest antigens. Interestingly, it was reported in a virology study, that HBcAg, expressed in *Xenopus* oocytes, was partially digested into smaller proteins upon incubation in trypsin: the main residue was a *circa* 17 kDa protein, but several intermediate forms ranging between 17 and 21 kDa were also detected, corresponding to different cleavage sites for trypsin at the C-terminus. The trypsin digestion did not seem to affect the particle assembly (Seifer and Standring, 1994). It is worth remembering that HBcAg bears in its monomeric structure a C-terminal tail arginine-rich domain. This domain is not essential for the assembly and stabilisation of the monomers into a VLP (Birnbaum and Nassal, 1990; Zheng et al., 1992). Intriguingly, it was demonstrated that the trypsin digests only these C-terminus sequences, which were “non-essential” for the particle assembly. The authors suggested that these C-terminal regions are accessible to the enzymatic attack, while other possible cleavage sites are relatively sequestered inside the VLP structure. Moreover, it was shown that the maximal trypsin cleavage was achieved after only 8 minutes of incubation (Seifer and Standring, 1994). The results obtained in SIF with pancreatin strongly suggest that the main pancreatic

524 enzyme involved in the digestion of HBcAg is trypsin. In fact the intestinal bio-relevant media
525 used determined a similar pattern of digestion to that indicated in the study, described by Saifer
526 and Standring (Seifer and Standring, 1994).
527
528 These results suggest that HBcAg VLPs, though partially digested, could still withstand the
529 intestinal environment while maintaining the particulate morphology and immunogenicity. In
530 fact, it was found that all the major epitopes mediating T- and B-cell responses are not found in
531 the C-terminal arginine rich region (Vanlandschoot et al., 2003), which is digested by the trypsin.
532
533 Despite the fact that pancreatic enzymes are the main proteases in the intestine, it has been
534 recently reported that pancreatic proteases only partially contribute to the total intestinal
535 enzymatic activity in animal models (Reuter et al., 2009). Therefore, the stability of HBcAg in
536 natural intestinal fluid (natIF) of the pig was investigated, in order to complement the *in vitro*
537 model. The whole pig small intestine was divided into four parts of approximately same length
538 and natIFs were collected from the resulting four sections and named natIF 1, natIF 2, natIF 3
539 and natIF 4 from the proximal to the distal regions. For evaluating the extent of digestion,
540 HBcAg VLPs were incubated in each of these natural media at 37 ºC for 4 hours and the fate of
541 HBcAg was subsequently evaluated.
542
543 Figure 6. shows the Coomassie stained SDS-PAGE, Western blot and dot blot of sucrose
544 gradient fractions. As a negative control, natIF diluted in water was used. Positive controls,
545 including a dilution of HBcAg in PBS and a dilution in previously boiled, and thus enzymatically
546 inactive, natIFs were used. The Coomassie stained gel (Figure 6. A) showed a faint 20 kDa band

547 corresponding to HBcAg in the positive control in PBS (lane 1). However, it was difficult to
548 identify HBcAg in the other samples containing natIFs due to the very high content of proteins of
549 various sizes present in these media and also visible in the negative control. Nevertheless, the
550 Western blot of the same samples (Figure 6. B) showed that anti-HBcAg immunoreactivity was
551 detected at *circa* 20 kDa in all positive controls where natIFs had been previously inactivated
552 (lanes 2 to 5). In contrast, for the actual digestion samples where active natIFs were present
553 (lanes 6 to 9), HBcAg was mainly visible as a *circa* 16-17 kDa band. The intensity of the band
554 was the highest in natIF 1 (lane 6) and reached a minimum in natIF 2 (lane 7), then it gradually
555 increased in natIF 3 (lane 8) and natIF 4 (lane 9). In natIF 4 a weak 20 kDa band was also
556 present, probably corresponding to intact HBcAg. As expected, no bands were seen in the
557 negative controls (lanes 11 to 14).
558
559 In a similar experiment samples were not boiled, so that the VLPs could maintain their native
560 physical structure. However, the enzymatic reaction was stopped at the end of the digestion study
561 by adding a protease inhibitor solution. Sucrose density gradient ultracentrifugation was then
562 carried out in parallel for the four samples, corresponding to the digestion of HBcAg in the four
563 natIFs, and for the control sample of HBcAg in PBS. After ultracentrifugation, fractions were
564 collected and analysed by dot blot. Figure 6. C shows that in the positive control anti-HBcAg
565 immunoreactive dots were found mainly in the 30 and 40 % w/v sucrose fractions, as typical for
566 intact HBcAg VLPs. For samples digested in the natIFs, HBcAg was still detected mainly in the
567 30 and 40% w/v sucrose density fractions; however, some immunoreactivity was also present in
568 the less dense fractions of the gradient.

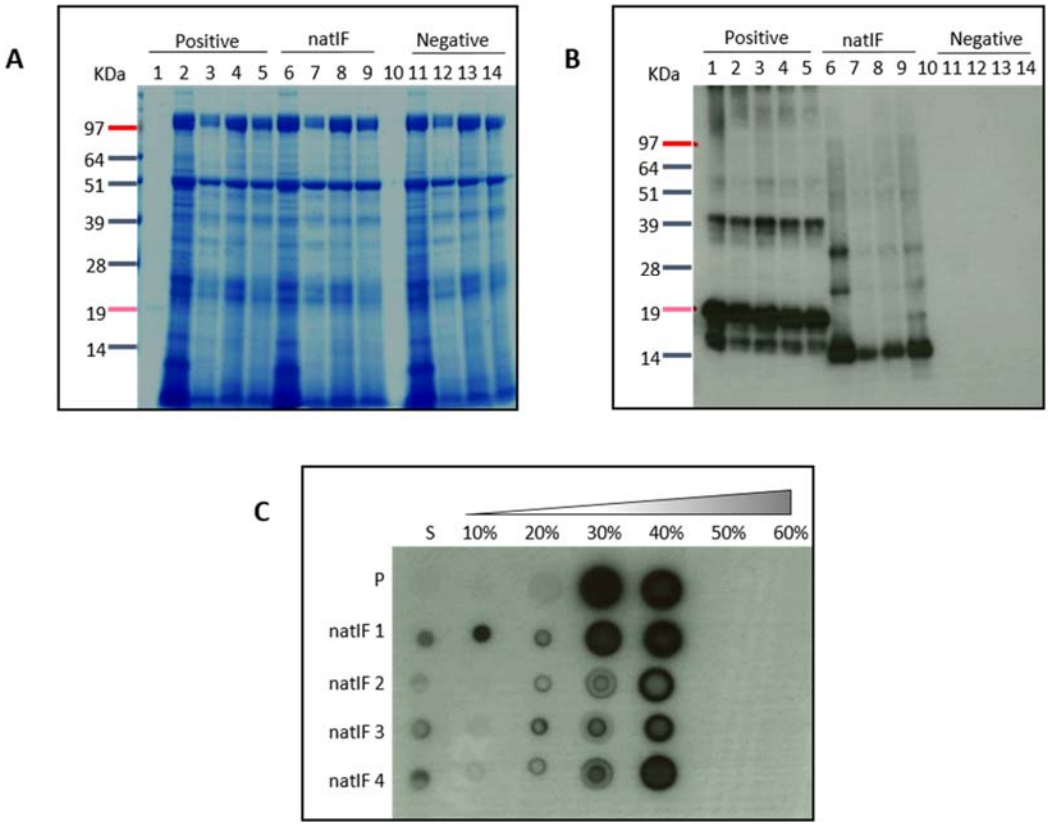

569

570 Figure 6. Ex vivo HBcAg stability in pig intestinal fluids. Stability studies were carried out in
571 four NatIFs collected from pig, named natIF 1, natIF 2, natIF 3, natIF 4 from the proximal to the
572 distal small intestine, respectively. HBcAg was incubated in each of the aforementioned media at
573 37 ºC for four hours. (A) and (B) represent the Coomassie stained SDS-PAGE and Western blot
574 (monoclonal antibody), respectively. The two gels were run identically: HBcAg in PBS (lane 1);
575 HBcAg in inactive natIF 1 to natIF 4 (lanes 2 to 5, respectively); HBcAg in natIF 1 to natIF 4
576 (lanes 6 to 9); empty lane (lane 10); PBS in natIF 1 to natIF 4 (lanes 11 to 14). (C) shows the dot
577 blot (monoclonal antibody) of fractions collected from sucrose density gradient
578 ultracentrifugation of different HBcAg samples incubated in each of the aforementioned natIFs.
579 The sucrose concentrations corresponding to density fractions collected are indicated

horizontally; the incubation samples analysed are indicated vertically. P = positive control (HBcAg in PBS); S = supernatant.

These results suggest that, despite the fact that the natural intestinal fluids have a much wider pool of proteases than just the pancreatic proteases used *in vitro* (Reuter et al., 2009), the main product of HBcAg digestion appears to be the same, i.e. a 16-17 kDa immunogenic protein still assembled as a VLP. In terms of physical stability of HBcAg in pig small intestinal fluids, the detection of some minor anti-HBcAg signal in the less dense fractions of the gradient suggested that partial disassembly took place upon incubation of HBcAg natIFs. However most of the immunoreactivity was still detected in the 30 and 40% w/v sucrose gradient fractions, where usually intact VLPs are found. It can be concluded that HBcAg appeared chemically unstable upon incubation in pig intestinal fluids. However, these data also suggest that the principal digestion products were still immunoreactive and that HBcAg was still mainly present as a VLP. The use of the pig natIFs here was part of a preliminary study to explore their use in the evaluation of the intestinal fate of administered pharmaceutical products. Here, the results of the pig natIF experiments were in line with those of the more conventional SIF experiments, suggesting that this approach has merit and agreeing with the previous work in this area by Wang et al (2015).

4. Conclusions

This study aimed to gain a better understanding of the stability of purified HBcAg in the gastro-intestinal (GI) tract: it was demonstrated that HBcAg VLPs were highly physically and chemically unstable in simulated human gastric media. Moreover, it was shown that HBcAg was

digested in simulated human intestinal fluid (SIF) and *ex-vivo* pig intestinal fluids, but surprisingly the main digested form of HBcAg maintained the particulate three-dimensional structure and the most antigenic epitopes. This offers an important prediction about the stability of HBcAg administered orally and can help interpret previous findings: previous research showed that HBcAg could elicit only weak immunogenicity upon oral administration in mice, hence it was speculated that exposure to the gastric environment could have resulted in either major chemical degradation or particulate disassembly before the VLP could enter into contact with the mucosal surfaces of the intestine (Huang et al., 2006). This assumption is supported by the current work, which indicates that HBcAg gastric instability, both in terms of chemical digestion and physical disassembly, can constitute a major obstacle to HBcAg oral delivery. The measured stability of HBcAg in SGF, SIF and natIFs in this study is likely to closely reflect its human *in vivo* stability, as it has recently been demonstrated that trends of digestion of peptide drugs in these media correlated well with their digestion in human fluids. The current findings are an important step towards understanding the complex oral immunogenicity of HBcAg. However, the current results also suggest that if the gastric instability could be bypassed, HBcAg could circulate through the human small intestine withstanding major degradation. Our current work is investigating this with a view to developing a patient-friendly orally-administered formulation which will protect the HBcAg from the harsh conditions in the stomach but release it intact in the intestine where it can exert its immunogenic effect.

Finally, in this paper a novel methodology to investigate the oral stability of VLPs has been put forward: the fate of the VLP was evaluated not only in terms of chemical digestion of the primary structure, but also in terms of the stability of the three-dimensional quaternary structure.

Acknowledgements

The authors would like to thank the University of East Anglia and the John Innes Centre (both Norwich Research Park) for funding this work as a PhD studentship for AB.

Declaration

The authors declare no competing financial interest.

References

Aljabali, A.A.A., Shukla, S., Lomonossoff, G.P., Steinmetz, N.F., Evans, D.J., 2012. CPMV-DOX Delivers. Mol. Pharm. 10, 3–10.

Ausar, S.F., Foubert, T.R., Hudson, M.H., Vedvick, T.S., Middaugh, C.R., 2006. Conformational stability and disassembly of Norwalk virus-like particles. Effect of pH and temperature. J. Biol. Chem. 281, 19478–88. doi:10.1074/jbc.M603313200

Birnbaum, F., Nassal, M., 1990. Hepatitis B virus nucleocapsid assembly: primary structure requirements in the core protein. J. Virol. 64, 3319–3330.

Broos, K., Vanlandschoot, P., Maras, M., Robbens, J., Leroux-Roels, G., Guisez, Y., 2007. Expression, purification and characterization of full-length RNA-free hepatitis B core particles. Protein Expr. Purif. 54, 30–37.

Crowther, R.A., Kiselev, N.A., Böttcher, B., Berriman, J.A., Borisova, G.P., Ose, V., Pumpens, P., 1994. Three-dimensional structure of hepatitis B virus core particles determined by electron cryomicroscopy. Cell 77, 943–950.

Evans, D.F., Pye, G., Bramley, R., Clark, A.G., Dyson, T.J., Hardcastle, J.D., 1988. Measurement of gastrointestinal pH profiles in normal ambulant human subjects. Gut 29, 1035–41.

649 Gomes, R.A.D.S., Batista, R.P., de Almeida, A.C., da Fonseca, D.N., Juliano, L., Hial, V., 2003.
650 A fluorimetric method for the determination of pepsin activity. Anal. Biochem. 316, 11–14.
651 doi:10.1016/S0003-2697(03)00025-3
652 Grgacic, E.V.L., Anderson, D.A., 2006. Virus-like particles: passport to immune recognition.
653 Methods 40, 60–5. doi:10.1016/j.ymeth.2006.07.018
654 Herbst-Kralovetz, M., Mason, H.S., Chen, Q., 2010. Norwalk virus-like particles as vaccines.
655 Expert Rev. Vaccines 9, 299–307. doi:10.1586/erv.09.163.Norwalk
656 Huang, Z., Elkin, G., Maloney, B.J., Beuhner, N., Arntzen, C.J., Thanavala, Y., Mason, H.S.,
657 2005. Virus-like particle expression and assembly in plants: hepatitis B and Norwalk
658 viruses. Vaccine 23, 1851–1858.
659 Huang, Z., Santi, L., LePore, K., Kilbourne, J., Arntzen, C.J., Mason, H.S., 2006. Rapid, high-
660 level production of hepatitis B core antigen in plant leaf and its immunogenicity in mice.
661 Vaccine 24, 2506–2513.
662 Jennings, G.T., Bachmann, M.F., 2008. The coming of age of virus-like particle vaccines. Biol.
663 Chem. 389, 521–536. doi:10.1515/BC.2008.064
664 Kalantzi, L., Goumas, K., Kalioras, V., Abrahamsson, B., Dressman, J.B., Reppas, C., 2006.
665 Characterization of the human upper gastrointestinal contents under conditions simulating
666 bioavailability/bioequivalence studies. Pharm. Res. 23, 165–76. doi:10.1007/s11095-005-
667 8476-1
668 Kammona, O., Kiparissides, C., 2012. Recent Advances in Nanocarrier-based Mucosal Delivery
669 of Biomolecules. J. Control. Release 161, 781–794. doi:10.1016/j.jconrel.2012.05.040
670 Lee, H.J., 2002. Protein drug oral delivery: the recent progress. Arch. Pharm. Res. 25, 572–84.
671 Lee, K.W., Tan, W.S., 2008. Recombinant hepatitis B virus core particles: association,

672 dissociation and encapsidation of green fluorescent protein. J. Virol. Methods 151, 172–80.
673 doi:10.1016/j.jviromet.2008.05.025
674 Mahato, R.I., Narang, A.S., Thoma, L., Miller, D.D., 2003. Emerging trends in oral delivery of
675 peptide and protein drugs. Crit. Rev. Ther. Drug Carrier Syst. 20, 153–214.
676 Mechtcheriakova, I.A., Eldarov, M.A., Nicholson, L., Shanks, M., Skryabin, K.G., Lomonossoff,
677 G.P., 2006. The use of viral vectors to produce hepatitis B virus core particles in plants. J.
678 Virol. Methods 131, 10–15.
679 Milich, D.R., Chen, M., Schödel, F., Peterson, D.L., Jones, J.E., Hughes, J.L., 1997. Role of B
680 cells in antigen presentation of the hepatitis B core. Proc. Natl. Acad. Sci. U. S. A. 94,
681 14648–53.
682 Milich, D.R., McLachlan, A., Moriarty, A., Thornton, G.B., 1987. Immune response to hepatitis
683 B virus core antigen (HBcAg): localization of T cell recognition sites within
684 HBcAg/HBeAg. J. Immunol. 139, 1223–31.
685 Newman, M., Suk, F.-M., Cajimat, M., Chua, P.K., Shih, C., 2003. Stability and Morphology
686 Comparisons of Self-Assembled Virus-Like Particles from Wild-Type and Mutant Human
687 Hepatitis B Virus Capsid Proteins. J. Virol. 77, 12950–12960. doi:10.1128/jvi.77.24.12950-
688 12960.2003
689 Peyret, H., 2015. A protocol for the gentle purification of virus-like particles produced in plants.
690 J. Virol. Methods 225, 59–63.
691 Peyret, H., Gehin, A., Thuenemann, E.C., Blond, D., El Turabi, A., Beales, L., Clarke, D.,
692 Gilbert, R.J.C., Fry, E.E., Stuart, D.I., 2015a. Tandem Fusion of Hepatitis B Core Antigen
693 Allows Assembly of Virus-Like Particles in Bacteria and Plants with Enhanced Capacity to
694 Accommodate Foreign Proteins. PLoS One 10.

695 Peyret, H., Stephen, S.L., Stonehouse, N.J., Rowlands, D.J., 2015b. History and Potential of
696 Hepatitis B Virus core as a VLP vaccine platform, in: Y, K., P, P. (Eds.), Viral
697 Nanotechnology. Boca Raton: CRC Press, pp. 177–186.
698 Reuter, F., Bade, S., Hirst, T.R., Frey, A., 2009. Bystander protein protects potential vaccine-
699 targeting ligands against intestinal proteolysis. J. Control. Release 137, 98–103.
700 doi:10.1016/j.jconrel.2009.03.015
701 Sainsbury, F., Lomonossoff, G.P., 2008. Extremely High-Level and Rapid Transient Protein
702 Production in Plants without the Use of Viral Replication. Plant Physioliogy 148, 1212–
703 1218. doi:10.1104/pp.108.126284
704 Sainsbury, F., Thuenemann, E.C., Lomonossoff, G.P., 2009. pEAQ: versatile expression vectors
705 for easy and quick transient expression of heterologous proteins in plants. Plant Biotechnol.
706 J. 7, 682–693.
707 Seifer, M., Standring, D.N., 1994. A protease-sensitive hinge linking the two domains of the
708 hepatitis B virus core protein is exposed on the viral capsid surface. J. Virol. 68, 5548–
709 5555.
710 Seitz, S., Urban, S., Antoni, C., Böttcher, B., 2007. Cryo-electron microscopy of hepatitis B
711 virions reveals variability in envelope capsid interactions. EMBO J. 26, 4160–7.
712 doi:10.1038/sj.emboj.7601841
713 Vanlandschoot, P., Cao, T., Leroux-Roels, G., 2003. The nucleocapsid of the hepatitis B virus: a
714 remarkable immunogenic structure. Antiviral Res. 60, 67–74.
715 Wang, J., Yadav, V., Smart, A.L., Tajiri, S., Basit, A.W., 2015. Toward Oral Delivery of
716 Biopharmaceuticals: An Assessment of the Gastrointestinal Stability of 17 Peptide Drugs.
717 Mol. Pharm. 12, 966–973. doi:10.1021/mp500809f

718 Whitacre, D., Lee, B., Milich, D.R., 2009. Use of hepadnavirus core proteins as vaccine
719 platforms. Expert Rev. Vaccines 8, 1565–1573. doi:10.1586/erv.09.121.Use
720 Wingfield, P.T., Stahl, S.J., Williams, R.W., Steven, A.C., 1995. Hepatitis core antigen produced
721 in Escherichia coli: subunit composition, conformational analysis, and in vitro capsid
722 assembly. Biochemistry 34, 4919–32.
723 Zheng, J., Schödel, F., Peterson, D.L., 1992. The structure of hepadnaviral core antigens.
724 Identification of free thiols and determination of the disulfide bonding pattern. J. Biol.
725 Chem. 267, 9422–9.
726